UV and IR Photoisomerization of Acetylacetone Trapped in a Nitrogen Matrix

A. Trivella, P. Roubin, P. Theulé, M. Rajzmann, and S. Coussan*

Laboratoire Physique des Interactions Ioniques et Moléculaires, UMR 6633, Université de Provence-CNRS, Centre St-Jérôme, 13397 Marseille Cedex 20, France

C. Manca

Physical Chemistry, ETH Zürich, CH8093 Zürich, Switzerland

Received: December 20, 2006; In Final Form: January 30, 2007

UV- and IR-induced photoisomerization of acetylacetone trapped in a nitrogen matrix at 4.3 K have been carried out using a tunable optical parametric oscillator type laser, or a mercury vapor lamp, coupled with Fourier Transform IR and UV spectroscopies. After deposition, the main form present in the cryogenic matrix is that chelated (enol). Upon UV irradiation, the intramolecular H bond is broken leading to nonchelated isomers among seven possible open forms. These forms have then been irradiated by resonant $\pi^* \leftarrow \pi$ UV irradiation, or by resonant ν_{OH} irradiation. The selective UV irradiation allows us to suggest a first vibrational assignment while the ν_{OH} irradiation leads us to observe interconversions between the nonchelated isomers. In order to support our vibrational assignment, we have carried out theoretical calculations at the B3LYP/6-311++G(2d,2p) level of theory. This study shows that only five isomers are observed among eight postulated.

I. Introduction

Acetylacetone (AA) is a β−diketone whose stable form in the gas phase is the enol form (Figure 1). It is one of the simplest molecules that exhibit symmetric ground state intramolecular proton transfer by proton-tunneling exchange between the two oxygen atoms. This proton transfer induced splitting has never been observed by matrix experiments; Barbara et al.[1] tried unsuccessfully to observe this tunneling in argon matrixes using Fourier Transform infrared (FTIR) and UV spectroscopies suggesting the splitting was not observed because of energy relaxation through the matrix phonons leading to the localization of the proton. The same conclusion was reached by our team for acetylacetone trapped in inert matrixes[2−5] such as nitrogen, argon, xenon, and neon.

The UV absorption of AA has been studied by Nagakura et al.[6] who identified a $\pi^* \leftarrow \pi$ transition at 38 020 cm^{-1} (ca. 263 nm) for the enol form, which has been confirmed both in a molecular beam by Yoon et al.,[7] who identified an absorption at 266 nm, and in a gas cell by Upadhyaya et al.[8] or more recently by Zewail et al.[9]

Among the theoretical studies, Dannenberg and Rios[10] estimated the H-bond strength of enolic-acetylacetone to be 12 kcal mol^{-1}, while Bauer and Wilcox tried to compare theoretical and experimental results. Delchev et al.[11−13] studied the energy barriers between the rotamers of both malonaldehyde and acetylacetone, and Došlić and Matanović[14] studied the IR spectroscopy of acetylacetone.

Actually, few experimental studies, as that of Nakata et al.,[15] to our knowledge, have been done on the photoinduced interconversion between the rotamers of acetylacetone coming from the fact that in gas phase promoting the first dipole allowed $\pi^* \leftarrow \pi$ transition around 265 nm only a fragmentation is observed.[7,8] Conversely, in matrixes, fragmentation is not observed,[16] and open rotamers are observed. Note that a cage
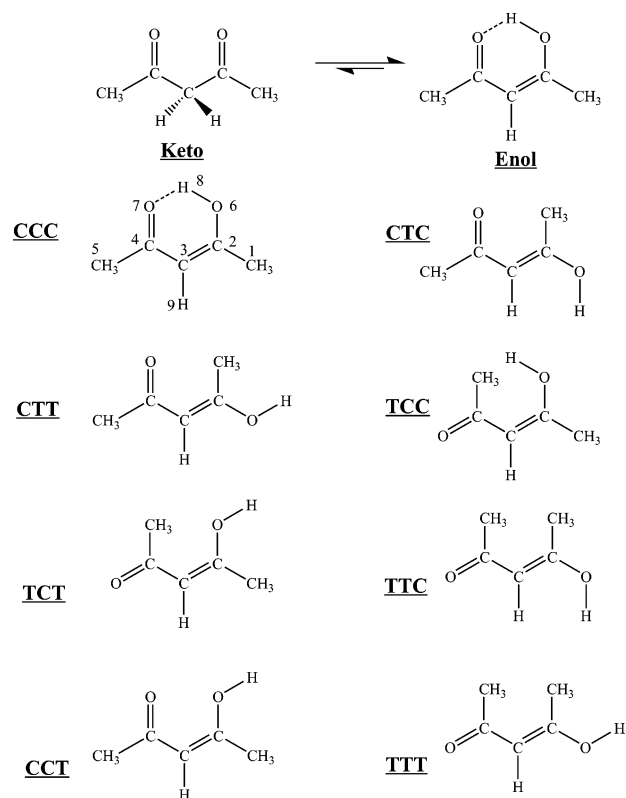

Figure 1. Keto−enol equilibrium. Scheme of the chelated (CCC) and of the 7 nonchelated forms (XXC or XXT) of the enol isomer. The structures are B3LYP/6-311++G(2d,2p) energetically ordered as follows CCC < CTC < CTT < ... < TTT (see Table 2).

effect could avoid fragments and favor the observation of isomerization.

Following our first experimental and theoretical study on the UV isomerization of acetylacetone,[16] which led to the identifica-

* Corresponding author. E-mail: coussan@up.univ-mrs.fr.

Acetylacetone Trapped in a Nitrogen Matrix

J. Phys. Chem. A, Vol. 111, No. 16, 2007 **3075**

TABLE 1: Calculated (Using the B3LYP/6-311++G(2d,2p) Formalism) Vibrational Frequencies (in cm⁻¹) of the Eight Isomers of Acetylacetone[a]

	CCC	CTC	CTT	TCC	TCT	TTC	CCT	TTT
ν_{OH}	3022.9	3797.3	3826.4	3808.6	3839.2	3801.6	3819.8	3836.0
	0.61	*0.08*	*0.15*	*0.16*	*0.16*	*0.09*	*0.14*	*0.16*
$\nu_{C=O}$	1643.3	1734.1	1738.6	1707.0	1704.0	1698.2	1751.0	1694.4
	0.36	*0.30*	*0.35*	*0.39*	*0.82*	*0.29*	*0.31*	*0.86*
$\nu_{C=C}$	1674.3	1635.6	1657.4	1667.0	1711.9	1671.2	1668.5	1703.3
	0.75	*1.00*	*0.68*	*0.70*	*0.05*	*0.78*	*0.72*	*0.04*
$\Delta\nu^b$	31.0	98.5	81.2	40.0	7.9	27.0	82.5	8.9
δ_{OH}	c	1230.8	1236.8	1325.9	1306.5	1220.8	1308.4	1211.3
		0.08	*0.26*	*0.08*	*0.32*	*0.44*	*0.53*	*0.43*
τ_{CH}	799.0	834.5	872.6	859.5	862.7	875.6	823.2	908.6
	0.06	*0.07*	*0.04*	*0.03*	*0.04*	*0.06*	*0.04*	*0.04*
τ_{OH}	1002.9	487.8	387.3	480.6	337.4	488.2	388.4	321.9
	0.12	*0.15*	*0.16*	*0.12*	*0.14*	*0.16*	*0.14*	*0.16*

[a] Relative band intensities are given in italics. [b] $\Delta\nu = |\nu_{C=O} - \nu_{C=C}|$ [c] See Table 6 (Supporting Information).

TABLE 2: Ground-State Energies of the Isomers of Acetylacetone (in kcal mol⁻¹) (a) Relative to the CCC Chelated Form and (b) Relative to the CTC Nonchelated Form as Obtained at the B3LYP/6-311++G(2d,2p) Level of Theory

	B3LYP/6-311++G(2d,2p)	
isomer	a	b
CCC	0.0	
CTC	11.1	0.0
CTT	11.8	0.7
TCC	12.7	1.6
TCT	13.6	2.5
TTC	14.3	3.2
CCT	15.6	4.5
TTT	16.6	5.5

tion of three isomer groups absorbing at three different UV wavelengths, we present here a complete study of the UV and IR isomerization of acetylacetone trapped in nitrogen matrixes leading to a complete vibrational assignment of the observed isomers of this molecule. We first present the theoretical study of the vibrational frequencies of each planar isomer (Figure 1) which is expected to be present in the cryogenic matrix, and then we present, using FTIR spectroscopy, the effects of successive UV and IR selective irradiation leading to the identification of the isomers present in the matrix.

II. Theoretical Vibrational Analysis

Minimum-energy structures of the enol chelated (CCC) and nonchelated forms (XXX, X = C or T) of acetylacetone were calculated at the B3LYP/6-311++G(2d,2p) level of theory. All calculations were performed using the Gaussian 98 program.[17]

Degrees of freedom were fully optimized without symmetry restrictions; normal coordinate calculations were carried out at each minimum-energy geometry for the S_0 electronic state. The resulting harmonic vibrational frequencies remained unscaled. The potential energy distributions (PED) of each form were calculated using the formalism developed by A. Allouche.[18,19] We have chosen to gather in Table 1 only the 6 most intense modes for which the different isomers present typical sets of bands.

In addition, Table 2 (and Table 4, Supporting Information) give the relative energies and the most relevant geometrical parameters for each of the eight isomers presented in Figure 1.

ν_{OH} **Mode.** The CCC ν_{OH} frequency is calculated at 3022.9 cm⁻¹ with a normalized intensity of 0.61; however, it is well-known that theoretical calculations do not take into account the H-bond effect on the intensities. Actually, because of the

strength of the H bond, the intensity of this mode is spread over hundreds of wavenumbers and is not therefore observed.[10]

The nonchelated forms can be separated into three groups: the first one, hereafter referred to as HF (High Frequency), contains TCT and TTT; the second one, hereafter referred to as MF (Medium Frequency), contains CTT, CCT, and TCC; and the last one, hereafter referred to as LF (Low Frequency), contains CTC and TTC. The average shift between these groups is 20 cm⁻¹ between HF and MF and 34 cm⁻¹ between HF and LF.

$\nu_{C=O}/\nu_{C=C}$ **Modes.** As in the case of the ν_{OH} region, the different isomers present typical sets of $\nu_{C=O}$ and $\nu_{C=C}$ bands which allow us to separate them into three groups: the first contains CTC, CTT, and CCT with $\Delta\nu$ ($\Delta\nu = |\nu_{C=O} - \nu_{C=C}|$) values of 98.5, 81.2, and 82.5 cm⁻¹, respectively. The $\nu_{C=C}$ mode of CTC is the most intense band among all the species (Table 1), and the $\nu_{C=O}$ bands of CTC and CTT are close (at 1734.1 and 1738.6 cm⁻¹, respectively); conversely, that of CCT is blue-shifted by 12.4 cm⁻¹ with respect to CTT, and its $\nu_{C=C}$ band is also blue-shifted by 11.1 and 32.9 cm⁻¹ with respect to CTT and CTC, respectively. Consequently, for isomers belonging to this group, we should observe a set of bands separated by about 80.0 cm⁻¹ and the two CCT bands blue-shifted by about 10.0 cm⁻¹ with respect to those of CTC.

The second group contains TCC and TTC with a $\Delta\nu$ of 40.0 and 27.0 cm⁻¹, respectively. The $\nu_{C=O}$ bands of TCC and TTC are respectively red-shifted, with respect to CTT, by 31.6 and 40.4 cm⁻¹, while the $\nu_{C=C}$ bands are blue-shifted by 9.6 and 13.8 cm⁻¹. These two isomers present $\nu_{C=O}$ and $\nu_{C=C}$ bands shifted apart by approximatively 33.0 cm⁻¹ and surrounded by those of the first group.

The third group contains TCT and TTT with a $\Delta\nu$ of 7.9 and 8.9 cm⁻¹, respectively. It should be noted that, as in the case of CCC, $\nu_{C=C}$ is at a higher frequency than $\nu_{C=O}$, whose calculated intensity is also weak. The $\nu_{C=O}$ mode is respectively red-shifted by 34.6 (TCT) and 44.2 (TTT) cm⁻¹ with respect to CTT, while the $\nu_{C=C}$ one is blue-shifted by 54.5 (TCT) and 45.9 cm⁻¹ (TTT). Therefore, the sets of the vibrational bands of these two isomers should present $\nu_{C=O}$ and $\nu_{C=C}$ bands shifted apart by approximatively 8.0 cm⁻¹ and surrounded by those of the first group.

δ_{OH} **Mode.** Similar to the above-described regions, we can conveniently divide the seven open isomers into two groups (Table 1). The first group contains CTC, CTT, TTC, and TTT, which present frequencies ranging between 1236.8 and 1211.3 cm⁻¹. The second group contains TCC, TCT, and CCT and presents higher frequencies, ranging between 1325.9 cm⁻¹ (TCC) and 1306.5 cm⁻¹ (TCT). The average shift between these two groups is 89 cm⁻¹.

τ_{CH} **Mode.** In this region excepted for CCC, calculated at 799.0 cm⁻¹, and TTT, calculated at 908.6 cm⁻¹, the other calculated τ_{CH} frequencies are all between 875.6 (TTC) and 823.7 (CCT) cm⁻¹ which could induce overlapping between the bands especially if they are broad. The only general behavior is that, in the pairs (XXC/XXT), the XXT partner presents the highest τ_{CH} frequency. One can also note that all of the intensities are weak with respect to those of the other regions described in this part.

τ_{OH} **Mode.** The CCC τ_{OH} mode is strongly blue-shifted by 590 cm⁻¹ with respect to those of the nonchelated forms because of the CCC delocalized π system, which stiffens this out-of-plane motion. We can separate once more the nonchelated isomers into three groups: the first one contains CTC, TCC, and TTC and exhibits frequencies centered around 485 cm⁻¹
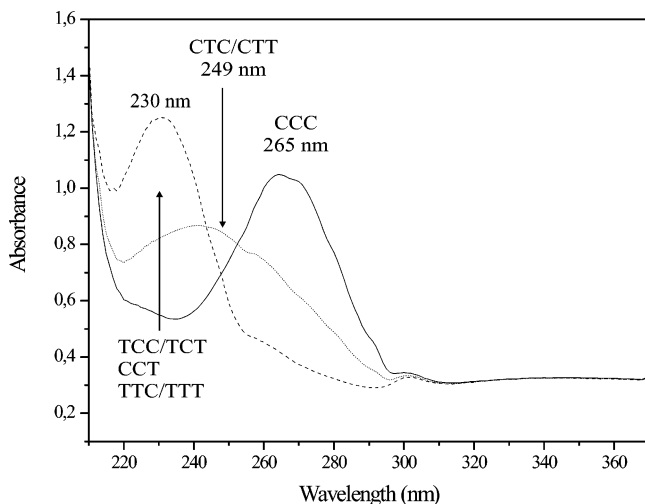
Figure 2. UV spectra of CCC and nonchelated forms (see text for labeling) recorded at 17 K on samples [AA/N_2] = 1/5000. The CTC/CTT and CCT/TCC/TCT/TTC/TTT bands were obtained after 45 and 90 min of laser irradiation at 265 nm, respectively.

while the second one includes CTT and CCT at 387.3 and 388.4 cm^{-1}, respectively, and the last one includes TCT and TTT at 337.4 and 321.9 cm^{-1}, respectively. Another interesting point is that the XXT partner of an XXC/XXT pair presents the lowest τ_{OH} frequency.

It is clear that the ν_{OH} and the $\nu_{C=O}/\nu_{C=C}$ regions are the most interesting for our vibrational assignment, because signals are intense and no strong overlapping bands are expected. Moreover, the different isomers present in these two regions present unambiguous sets of bands or shifts. We will focus our attention on these two regions, whereas that of the δ_{OH} mode will be a good check for the assignment. This vibrational analysis is a really useful support in the assignment of the isomers created by UV irradiation and interconverted by resonant ν_{OH} IR irradiation.

III. Experimental Methods

AA vapor (Aldrich-Chemie, $C_5H_8O_2$ > 99% percent purity) distilled under vacuum and nitrogen gas (Air Liquide, N60 grade) were mixed in ratio AA/N_2 = 3/1000 (IR spectroscopy) and AA/N_2 = 1/5000 (UV spectroscopy) in a vacuum line using standard manometric techniques. Different experimental setups have been used both in Paris (laboratory LADIR UMR 7075 of the University Pierre et Marie Curie) and in Marseille. The mixture was sprayed onto either a CsI window or a highly polished Ni-plated or Au-plated copper cube maintained at 17 K by closed-cycle helium cryostats (CTI-Cryophysics or Cryomech PT-405, Marseille; Air Products CSW 202, Paris). The IR spectra were recorded at 10 and 4.3 K in the transmission–reflection mode using three different interferometers; spectra between 4000 and 20 cm^{-1} were recorded at 10 K with a Bruker 120 FTIR spectrometer equipped with InSb, MCT, and bolometer detectors (Paris). Spectra between 4500 and 500 cm^{-1} were recorded at 10 K with a Nicolet 7000 and were recorded at 4.3 K with a Bruker IFS 66/S spectrometer equipped with MCT detectors (Marseille). All of the spectra were recorded with a 0.1 cm^{-1} resolution. UV spectra (Figure 2) were recorded at 17 K in the transmission mode using a SAFAS 190 DES spectrometer. Two irradiation sources were used: an Oriel high-pressure 200 W mercury lamp (Paris, Marseille) and a pulsed (10 Hz, 15 ns), tunable UV–visible–IR OPO BMI-Thalès laser (Marseille, average power: UV, 8 mW; IR, 10 mW; FWHM ≤4 cm^{-1}).

IV. Results and Discussion

With a dilution AA/N_2 = 3/1000, the signals in the whole spectral range are assignable to the monomers.[20]

A. UV Irradiation. *1. CCC Selective Irradiation at 265 nm.* This irradiation opens the pseudo-cycle of CCC: the nonchelated isomers grow as seen in the ν_{OH} and $\nu_{C=O}/\nu_{C=C}$ regions (Figure 3a). The IR spectrum also shows that maintaining the irradiation on CCC induces the decrease of the ν_{OH} bands centered at 3607.0, 3593.5, 3591.3, 3587.5, 3586.0, and 3583.1 cm^{-1} (Figure 3b). As evidenced by the UV spectra displayed in Figure 2, the 265 and 249 nm bands overlap, and a selective 265 nm irradiation also irradiates the "red side" of the 249 nm band, inducing further interconversion between open forms.[16]

2. CTC/CTT Selective Irradiation at 255 nm. As it can be seen in Figure 3c, the 255 nm irradiation provokes the same effects as those observed in the case of a prolonged 265 nm irradiation. In the ν_{OH} region, the LF bands plus an additional 3607 cm^{-1} band decrease, while in the $\nu_{C=O}/\nu_{C=C}$ region two sets of bands separated by approximatively 90 cm^{-1} also decrease. CTC and CTT have theoretically predicted ν_{OH} bands and $\nu_{C=O}/\nu_{C=C}$ shifts (Table 1) which match the experimental ones. However, CCT presents a predicted MF ν_{OH} frequency and $\nu_{C=O}/\nu_{C=C}$ shift which also fit those observed. It does not allow us to strictly discard this candidate. Moreover, CCT and TCC are calculated to be on the "red side" of the 5 last open-forms $\pi^* \leftarrow \pi$ transition band, centered at 230 nm;[16] these two species can then be irradiated upon a 255 nm irradiation once the 249 nm band is weak enough (Figure 2). Consequently a first hypothesis is that the decreasing band observed at 3607 cm^{-1} could be assigned to CCT or TCC. However, no $\Delta\nu$ of 40 cm^{-1} for the decreasing bands is observed. This latter argument is proof that the 3607 cm^{-1} band could not be assigned to TCC. On the other hand, there is also a strong argument against the assignment of this band to CCT: we do not observe $\nu_{C=O}$ and $\nu_{C=C}$ modes blue-shifted by about 17 and 33 cm^{-1} with respect to CTC, respectively (Table 1). With regard to the increases observed in the $\nu_{C=O}/\nu_{C=C}$ region, the differences are between 48 and 5 cm^{-1} which can correspond to TCC, TCT, TTC, or TTT.

Carrying out this irradiation, we have been able to give the vibrational assignment of CTC and CTT species but without being able to unambiguously discriminate between them; we will improve this assignment by carrying out selective IR irradiation. With regard to the rest of the nonchelated forms, it has been impossible at this stage to make a definitive vibrational assignment.

3. CCT/TCC/TCT/TTC/TTT Selective Irradiation at 230 nm. The most salient result of the 230 nm irradiation is the back-isomerization of the nonchelated forms toward that chelated (Figure 3d). However, one should note that this back-isomerization is never complete. A small amount of nonchelated forms remains even after a long UV irradiation at 230 nm. It is certainly due to the overlap with the "blue side" of the 265 nm band, CCC being irradiated when the 230 nm UV band has quite vanished, provoking mainly the resurgence of the CTC/CTT pair and therefore a photostationary equilibrium CCC ⇆ CTC/CTT. This irradiation does not bring any determining insights for a better vibrational assignment of the nonchelated species because they are irradiated all together.

Concerning the FIR part of the spectra, we only observe three CCC bands located at 398.2, 359.1, and 221.0 cm^{-1} tentatively assigned to the δ_{CCC}, coupled δ_{CCC}/ν_{CC}, and δ_{CCC} modes, respectively. With regard to the open forms, as shown
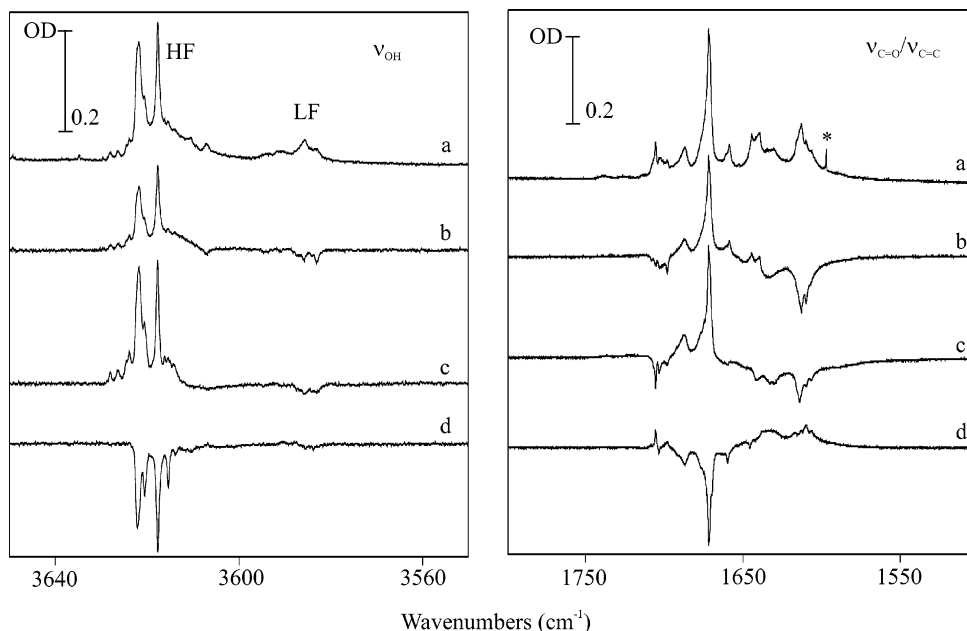
Figure 3. IR spectra in the ν_{OH} and $\nu_{C=O}/\nu_{C=C}$ regions of samples $[AA/N_2] = 3/1000$, at 4.3 K. (a) After 104 min irradiation at 265 nm, (b) difference after 104 min irradiation at 265 nm minus after 53 min laser irradiation at 265 nm, (c) difference after minus before 57 min irradiation at 255 nm, and (d) at 4.3 K, difference after minus before 38 min irradiation at 230 nm. HF, LF (high frequency, low frequency). *:ν_2 mode of water.

in Table 3, all the bands are weak and overlapped rendering their assignments ambiguous.

4. Thermal Effects After UV Irradiation. We have observed thermal effects by annealing between 17 and 28 K after selective or broad band UV irradiation. This leads to the vanishing of unstable sites and to more structured IR spectra. Indeed, considering the large geometrical changes occurring upon UV irradiation, one can suggest that the chelated trapping sites have been distorted leading to stable and unstable nonchelated sites. All of these thermal effects can be understood in terms of matrix rearrangements which make the less stable trapping sites almost vanish. Depending on the annealing temperatures and on the history of the matrixes, we find the exchanges between sites present subtle behaviors.

The most salient information we can then retrieve from these thermal effects is that we do not observe back conversions nonchelated → chelated form as it is clear, for example, by the two isolated CCC bands located at 1262.5 and 1249.5 cm^{-1} which do not grow upon annealing. CCT and TCC are expected to have the lowest energy barriers to go to CCC (by single rotations around C—O and C—C, respectively). The fact that we do not observe this thermally induced back isomerization raises the following question: are these two species present in the matrix or is the thermal energy not enough to get over the barrier and relax to CCC ? At this stage, we are unable to answer. One more idea is that we also do not observe any intra pair (XXC/XXT) interconversions and this raises a question concerning the C—O internal rotation barrier height.

B. IR Irradiation. In order to probe whether ν_{OH} photons have enough energy to induce interconversions between the nonchelated forms or to induce the back conversion from CCT or TCC toward CCC, we have carried out selective IR irradiation and observed effects mainly at 3622/3612 and 3588 cm^{-1}. These irradiation results, detailed below, are really helpful to discriminate the isomers present in the matrix and to deepen our previous vibrational assignment.

1. Irradiation at 3588 cm^{-1}. This irradiation, performed after a broad-band UV irradiation, is displayed in Figure 4 in the

ν_{OH}, $\nu_{C=O}/\nu_{C=C}$, and $\delta_{OH}/\nu_{CO}/\nu_{CC}$ regions. It is worth noticing that the globar source of the FTIR spectrometer also induces isomerization; it leads although much slower to the complete recovering of the initial state after 15 h (Figure 4c).

In the ν_{OH} region, we observe the decrease of all of the LF bands: three intense at 3587.5, 3586.7, and 3585.7 cm^{-1} and four weak located at 3594.9, 3594.0, 3593.5, and 3591.3 cm^{-1}. These decreases are counterbalanced by the growth of not less than nine bands spread over the HF and MF regions and centered at 3623.1, 3622.0, 3620.5, 3619.1, 3615.4, 3613.2, 3610.5, 3607.4, and 3606.9 cm^{-1}.

In the $\nu_{C=O}/\nu_{C=C}$ region, two intense doublets are decreasing at 1703.3−1702.6 and 1615.5−1614.2 cm^{-1}, the latter showing a shoulder at 1610.8 cm^{-1}, together with weak bands at 1698.8−1698.1, 1694.8, 1673.2, and 1659.8 cm^{-1}. The observed increases in this region are mainly those of an intense quadruplet located at 1707.7−1707.0−1706.4−1705.5 and of four overlapping broad bands at 1641.9, 1634.9, 1633.1, and 1629.7 cm^{-1}. In order to clarify the description in this region, we will consider the $\Delta\nu$ between these main bands. We do not consider the three bands at 1698.8−1698.1 and 1694.8 cm^{-1} which are due to different trapping sites as it is confirmed by annealing the sample. Upon this irradiation, the two main bands separated by 88.1 cm^{-1} are decreasing while the two other ones separated by 71.7 cm^{-1} are increasing. As it will be seen in the next section, the changes observed for the weak bands located at 1673.2 and 1659.8 cm^{-1} are due to minor globar effects which allows us to not address them.

In the $\delta_{OH}/\nu_{CO}/\nu_{CC}$ region, the main changes can be described as an intensity inversion between two close signals at 1162.3 cm^{-1}, presenting a shoulder at 1165.3 cm^{-1} which is decreasing, and a triplet at 1157.7−1157.2−1156.2 cm^{-1} which is increasing. Together with these intense spectral changes, one observes weak bands decreasing at 1279.2, 1215.2, 1210.7, and 1208.0 and a doublet at 1179.0−1177.9 cm^{-1}, while weak bands located at 1281.3, 1263.5, 1232.1, 1227.6, 1224.9, 1220.8−1219.8, 1216.8, and 1212.7 cm^{-1} are increasing.

TABLE 3: Experimental Vibrational Frequencies (cm⁻¹) of the Isomers of Acetylacetone Trapped at 4.3 K in a Nitrogen Matrix

approximate description	ν_{exp} (cm⁻¹)				
	CCC	CTC	CTT	TCT	TCC
ν_{OH}	n.o.[a]	3594.9, w	3623.1, w, sh	3627.7, w	3614.0, m, sh
		3594.0, w	3619.1, w, sh	3626.3, w	3611.8, m, br
		3593.5, w	3615.4, w, sh	3624.5, w, sh	
		3591.3, w	3613.2, m	3622.0, s	
		3587.5, m	3610.5, m	3620.7, s, sh	
		3586.7, m, sh	3607.4, w, sh	3618.8[b]	
		3585.7, m	3606.9, w, sh		
ν_{CH}	3013.3, w	3018.3, w	3035.5, w	3004.0, w	2997.7, w
	2977.9, w	3009.3, w	2925.1, w	2983.1, w	2967.4, w
	2939.1, w	2975.3, w		2927.9, w	2937.5, w, sh
	2933.7, w	2968.4, w			2921.8, w, sh
		2935.7, w			
		2932.4, w			
$\nu_{C=O}$	1614.4, s, br	1703.3, m	1707.7, m	1670.8, s	1673.1, s, sh
		1702.6, m	1707.0, m	1669.4, s, sh	1672.0, s, sh
		1698.8, w	1706.4, m		1671.6, s, sh
		1698.1, w	1705.5, m		1658.8, w, sh
		1694.8, w			
$\nu_{C=C}$	1636.0, s, br	1615.5, s	1641.9, m, br	1687.6, m, br	1648.2, w
		1614.2, s	1634.9, m, sh	1676.6, m, br, sh	1643.2, w, sh
			1633.1, m, sh		1640.5, m, sh
			1629.7, m		1639.6, m
$2\tau_{CH}$?	1539.1, w				
δ_{CH_3}	1462.2, m	1442.4, w, br	1453.0, w	1434.2, w	1454.0, w, br
	1438.4, sh	1439.6, w, sh	1429.2, m, br, sh	1422.6, m, br	1450.3, w, br
	1431.7, sh	1426.3, m	1406.6, m	1421.5, m, sh	1444.7, m, br
	1424.0, s	1425.5, m	1404.5, m	1420.3, w, sh	1405.0, w, br
	1377.0, w	1423.7, m, sh	1371.8, w, br	1391.5, m, sh	1398.6, m
	1374.3, w	1368.2, m, sh	1363.5, m, sh	1389.9, m, br	1398.1, m
	1362.0, s[c]	1365.6, m	1361.2, m	1388.9, m, sh	1396.9, m
	1361.1, sh, s[c]	1355.8, m	1352.9, m	1367.4, m, br	1358.1, w, sh
	1359.0, s[c]			1366.1, w, sh	1355.9, m, br
				1348.2, w, sh	1355.6, m, sh
				1347.7, w, br	1352.8, w, br
				1346.3, w, sh	1352.4, w, sh
				1345.6, w, br	
$\delta_{OH}/\nu_{CC}/\nu_{CO}/\delta_{CCH}$	1326.4, w, br	1279.2, w	1281.3, w	1295.3, w, sh	1257.7, m
	1310.2, w, br	1215.2, w	1263.5, w	1290.2, w, sh	1127.2, m
	1289.8, w, br	1210.7, w	1232.1, w	1286.8, m, sh	1125.0, m
	1273.2, w, br	1208.0, w	1227.6, w	1283.4, w, sh	
	1250.1, m	1179.0, w	1224.9, w	1263.3, m	
	1171.2, w, br	1177.9, w	1220.8, w	1262.0, m	
		1165.3, m, sh	1219.8, w		
		1162.3, m	1216.8, w		
			1212.7, w		
			1157.7, m, sh		
			1157.2, m		
			1156.2, m		
$\tau_{OH}/\tau_{CH}/\nu_{CC}/\nu_{CO}/r_{CH_3}$[d]	1026.5–1025.0, w	1011.9, w	945.1, w	1025.3, w	1018.8, m
$\tau_{CH}/\nu_{CC}/\nu_{CO}/r_{CH_3}$[e]	1016.9–1014.0, w	983.4, w	942.8, w	1024.3, w, sh	1016.1, m
	997.7, w	970.6, w	940.8, w	995.8, m	985.4, m
	961.2, w	946.2, w	855.5, w	995.2, m, sh	984.6, m, sh
	954.5, w, sh	941.6, w	847.5, w	913.7, m	926.8, w
	950.1, w, sh	936.8, w	844.7, w	891.3, w	897.9, w, br
	949.1, w, sh	838.4, w	843.4, w	835.2, w	828.2, w, sh
	945.4, w	837.2, w	842.2, w	832.1, w	
	943.1, w	836.5, w	841.6, w	830.0, w	
	938.3, w	819.1, w	834.2, w	829.3, w	
	910.1, w, br	817.3, w	831.7, w	811.9, w, br	
	786.4, w	815.6, w			
	780.6, w	812.9, w			
	776.9, w				
	775.9, w				
	773.2, w, sh				
	771.9, m				
$\nu_{CC}/\delta_{CCO}/\delta_{CCC}$[d]	644.9, w	626.2, w	632.5, w	592.9, w	530.4, w
$\tau_{OH}/\nu_{CC}/\delta_{CCO}/\delta_{CCC}$[e]	634.9, w		629.0, w		
	519.2, w			nonchelated[f]	
	508.7, w	589.7	502.6	482.9	424.3

Acetylacetone Trapped in a Nitrogen Matrix

J. Phys. Chem. A, Vol. 111, No. 16, 2007 **3079**

TABLE 3: (Continued)

				ν_{exp} (cm^{-1})			
approximate description	CCC				nonchelated^f		
397.4 (?), w	575.8	524.2	476.8	420.1			
221.0 (?), w, br	537.3	499.9	445.5	415.1			
	531.5	491.4	439.4	406.6			
	528.8	487.1	437.0	398.7			
	524.2	486.0	429.7				

^{a} n.o.: non-observed; s, strong; m, medium; w, weak; br, broad; sh, shoulder. ^{b} Tentatively assigned to TCT. ^{c} Coupled mode: $\nu_{C=C}^5(39)/\nu_{CO}^6(20)/\delta_{COH}^{36}(20)/\nu_{C=O}^{10}(16)$ (see Supporting Information). ^{d} Chelated. ^{e} Nonchelated. ^{f} This list is given for all the nonchelated forms present in the matrix. All these bands are weak.
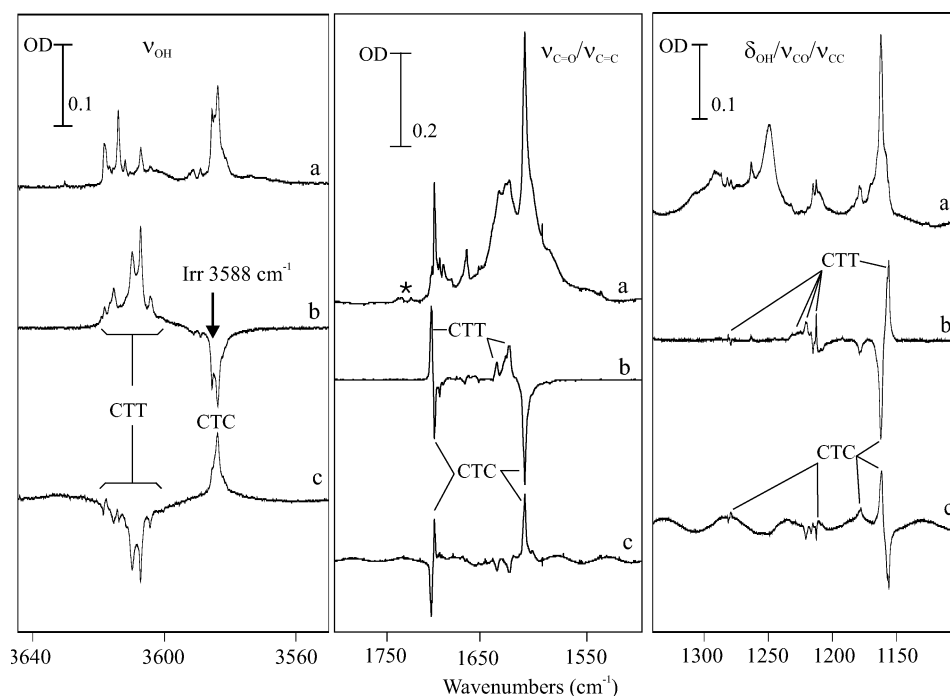

Figure 4. IR irradiation of a sample [AA/N$_2$] = 3/1000. ν_{OH}, $\nu_{C=O}/\nu_{C=C}$, and $\delta_{OH}/\nu_{CO}/\nu_{CC}$ regions of spectra recorded at 4.3 K (a) before irradiation, (b) difference after minus before 42 min irradiation at 3588 cm^{-1}, and (c) same as b for 15 h irradiation by the globar. *Diketone.

Considering only these three regions, we have to identify which isomers are matching these frequencies and are able to be interconverted upon this IR irradiation. The photoisomerized species have an LF ν_{OH} band, a $\Delta\nu$ of 88.1 cm^{-1} in the $\nu_{C=O}/\nu_{C=C}$ region, and an intense band around 1162.3 cm^{-1}. CTC is the only candidate which matches these vibrational bands. The photoproduct present HF or MF ν_{OH} bands, a $\Delta\nu$ of 71.7 cm^{-1} in the $\nu_{C=O}/\nu_{C=C}$ region, and an intense band around 1157.0 cm^{-1} in the $\delta_{OH}/\nu_{CO}/\nu_{CC}$ one. Considering that a ν_{OH} photon can induce a rotation only around single bonds, we find it clear that the photoproduct can only be CTT obtained from CTC by a rotation around the C−O bond. Other important insights can also be retrieved from this irradiation: despiteTTC presenting a LF ν_{OH} band, the fact that all the LF bands are decreasing upon this irradiation provides proof that all these bands are due to CTC. This allows us therefore to discard the presence of TTC in the matrix. Another point is the multiplicity of the ν_{OH} bands observed for CTT, which could lead to a certain confusion. Actually, they are all clearly due to this isomer except those at 3622.0 and 3620.5 cm^{-1}, as it will be proved in the next section. The last point has to deal with the bands we observe in the $\delta_{OH}/\nu_{CO}/\nu_{CC}$ region. According to the PED results (see Supporting Information), the only mode which is calculated to be intense for both CTC and CTT is ν_{CC}/δ_{CCH}; therefore, we suggest to assign the bands at 1162.3 and 1157.7−1157.2−

1156.2 cm^{-1} to CTC and CTT, respectively. We suggest to assign the weak bands at 1279.2 and 1281.3 cm^{-1} to the ν_{CO} mode of CTC and CTT, respectively, while those at 1215.2, 1210.7, and 1208.0 cm^{-1} should be assigned to the δ_{OH} mode of CTC, and those at 1232.1, 1227.6, 1224.9, 1220.8−1219.8, 1216.8 and 1212.7 cm^{-1} should be assigned to CTT, respectively; the multiplicity of signals arises from the multiplicity of trapping sites. Finally, the decreasing CTC doublet at 1179.0−1177.9 cm^{-1} is most probably due to a site, and the band at 1263.3 cm^{-1} is that of an isomer which is not directly involved in this photoconversion.

Carrying out this irradiation at 3588 cm^{-1}, we have provided proof for the photoconversion between CTC and CTT, which has led to the respective identification of two isomers (Table 3).

2. Irradiation at 3622 and 3612 cm^{-1}. The changes occurring upon irradiation, carried out after a UV selective irradiation at 265 nm, are displayed in Figure 5b and c in the ν_{OH}, $\nu_{C=O}/\nu_{C=C}$, and $\delta_{OH}/\nu_{CO}/\nu_{CC}$ spectral regions.

We mainly observe the decrease of ν_{OH} bands located at 3622.0, 3620.5, and 3618.8 cm^{-1} while only one broad signal, presenting shoulders at 3614.0 and 3611.8 cm^{-1}, is growing. We also observe the decrease of weak bands located at 3627.7, 3626.3, and 3624.5 cm^{-1} and a very weak increase of the broad CTC band at 3585.7 cm^{-1}. This last fact is clearly due to the
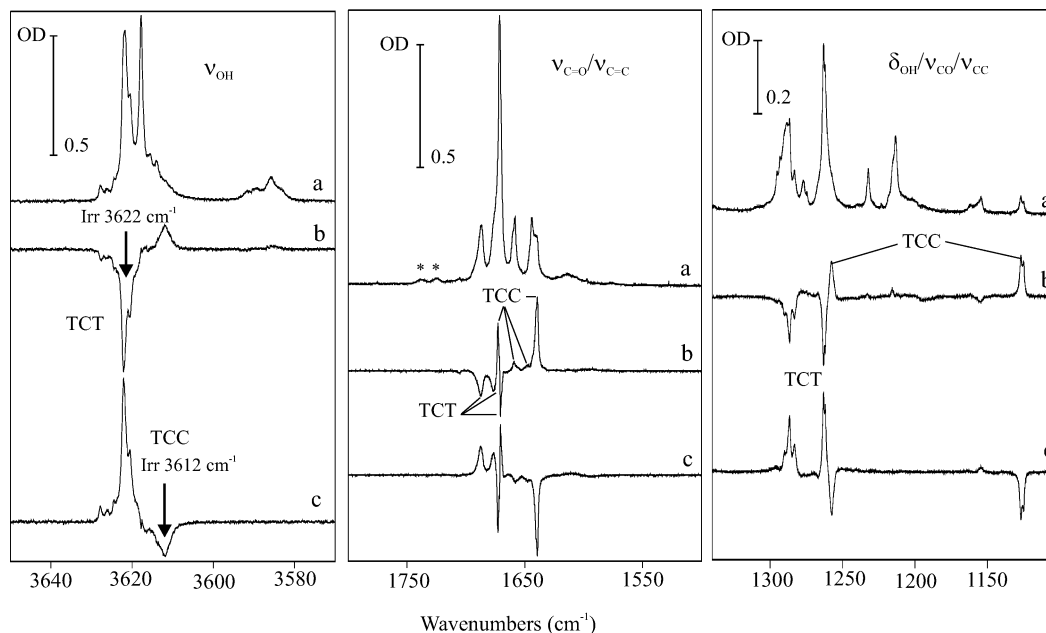
Figure 5. IR irradiation of a sample [AA/N$_2$] = 3/1000. ν_{OH}, $\nu_{C=O}/\nu_{C=C}$ and $\delta_{OH}/\nu_{CO}/\nu_{CC}$ regions of spectra recorded at 10 K (a) before irradiation, (b) difference after minus before 11 min irradiation at 3622 cm^{-1}, and (c) same as b for 18 min irradiation at 3612 cm^{-1}.* Diketone.

irradiation of one site of CTT which is present in a small quantity after the UV selective irradiation, as described above.

In the $\nu_{C=O}/\nu_{C=C}$ region, one observes the decrease of two bands located at 1687.6 and 1676.6 cm^{-1} and of a doublet at 1670.8−1669.4 cm^{-1} while an intense triplet at 1673.1−1672.0−1671.6, an intense band at 1639.6 cm^{-1}, and to a much less extent three weak bands at 1658.8, 1648.2, and 1643.2 cm^{-1} are growing. In parallel, one observes a weak conversion between CTT at 1706.4 and CTC at 1614.2 cm^{-1}. As already reported in the case of the former irradiation at 3588 cm^{-1}, we can summarize the effects in this region by the decrease of bands separated by 16.8, 11.0, or 5.8 cm^{-1} while the main increases are separated by 33.5 cm^{-1}. In addition, the weak increases are separated by 15.6, 10.6, or 5.0 cm^{-1}.

In the $\delta_{OH}/\nu_{CO}/\nu_{CC}$, one mainly observes the decrease of a triplet located at 1290.2, 1286.8, and 1283.4 cm^{-1} presenting a shoulder at 1295.3 cm^{-1}, concomitantly with that of a doublet at 1263.3−1262.0 cm^{-1}. These decreases are counterbalanced by two intense increases at 1257.7 cm^{-1} and a doublet at 1127.2−1125.0 cm^{-1}. In parallel, as for the $\nu_{C=O}/\nu_{C=C}$ region, one also observes weak spectral changes between 1275 and 1150 cm^{-1} due to CTC (increasing bands) and CTT (decreasing bands).

In this case, the parent isomer presents a HF ν_{OH} mode, a $\Delta\nu$ in the $\nu_{C=O}/\nu_{C=C}$ region between 16.8 and 5.8 cm^{-1}, and two intense bands around 1287 cm^{-1}. Considering the fact that we have already identified CTC and CTT and discarded the possibility of the presence of TTC, the isomers which fulfill all of these conditions are TCT and TTT. In fact, although the TTT ↔ TTC isomerization is likely to be observed by IR irradiation, we do not observe any spectral evidence for this reaction: this can be explained by the TTT syn-1,3 destabilizing interaction which rapidly induces the TTT → TTC reaction during the relaxation processes. The photoproduct ν_{OH} mode is red shifted by 10 cm^{-1} with respect to that of TCT; in the $\nu_{C=O}/\nu_{C=C}$ region, its $\Delta\nu$ is about 33.5 cm^{-1} and displays in the $\delta_{OH}/\nu_{CO}/\nu_{CC}$ region two bands located around 1258.0 and 1126.0 cm^{-1}, thus separated by 122.0 cm^{-1}. The only possible candidate is TCC: this is in good agreement with the two bands in the ν_{CC} and the $\nu_{CC}/\nu_{CO}/\delta_{COH}$ regions calculated at 1280.2 and 1145.5 cm^{-1},

which lead to a difference of 134.7 cm^{-1}. Carrying out the back irradiation at 3612 cm^{-1}, we recover exactly the initial state indicating a reversible reactional pathway.

Carrying out these irradiation at 3622 and 3612 cm^{-1}, we have put into evidence the photoconversion between TCT and TCC, which has led to the identification of these two isomers (Table 3).

V. Conclusion

UV and IR selective irradiation have been performed on acetylacetone isolated in a cryogenic nitrogen matrix and have enabled us to give a vibrational assignment for five isomers out of eight, namely, the two open-form pairs CTC/CTT and TCC/TCT. IR spectral evidence has not been found for CCT nor for the couple TTC/TTT. These last three species have been calculated by DFT to be the less stable among the open forms: the strong electronic repulsion between the sp^2 and the sp^3 electronic pairs of the two oxygen atoms (CCT) or the syn-1,3 destabilizing interaction between the two methyl groups (TTC/TTT) makes them less stable. They certainly relax too quickly toward more stable species to be observed within the time scale of our experiment.

Beyond these spectral identifications, we have also retrieved some information about the reactional pathways: we did observe isomerization between CCC and the open forms uniquely by UV irradiation which is consistent with the high barrier to conversion because of the strength of the H bond. These isomerizations certainly take place in upper excited electronic states. However, if we consider the open form TCC obtained from CCC by single rotation around C−C, the fact we observe no back reaction toward CCC by IR selective irradiation in the ν_{OH} region indicates that in our experimental conditions the only reactional pathway in which this species is involved is the one leading to TCT. Reciprocally from this latter isomer, the only isomer formed by IR irradiation or annealing is TCC. The same behavior is noticed in the case of the other couple CTC/CTT, showing only isomerization around C−O upon IR irradiation or annealing. Actually, there is only one reactional pathway involving a rotation around C−C that could occur between

Acetylacetone Trapped in a Nitrogen Matrix

J. Phys. Chem. A, Vol. 111, No. 16, 2007 **3081**

identified species, that is, CCC ↔ TCC, the others leading to CCT, TTC, or TTT which we do not observe. Finally, the reactional pathways involved in the isomerization between the chelated and the nonchelated forms are currently under study in our laboratory and will be reported in a forthcoming publication.

Supporting Information Available: Geometric parameters of each isomer in Figure 1, internal coordinates, and calculated frequencies. This material is available free of charge via the Internet at http://pubs.acs.org.

References and Notes

(1) Firth, D. W.; Barbara, P. F.; Trommsdorff, P. *Chem. Phys.* **1989**, *136,* 349.

(2) Roubin, P.; Chiavassa, T.; Verlaque, P.; Pizzala, L.; Bodot, H. *Chem. Phys. Lett.* **1990**, *175,* 655.

(3) Chiavassa, T.; Roubin, P.; Pizzala, L.; Verlaque, P.; Allouche, A.; Marinelli, F. *J. Phys. Chem.* **1992**, *96,* 10659.

(4) Chiavassa, T.; Verlaque, P.; Pizzala, L.; Allouche, A.; Roubin, P. *J. Phys. Chem.* **1993**, *97,* 5917.

(5) Chiavassa, T.; Verlaque, P.; Pizzala, L.; Roubin, P. *Spectrochim. Acta, Part A* **1994**, *50,* 343.

(6) Nakanishi, H.; Morita, H.; Nagakura, S. *Bull. Chem. Soc. Jpn.* **1977**, *50,* 2255.

(7) Yoon, M. C.; Choi, Y. S.; Kim, S. K. *J. Chem. Phys.* **1999**, *110,* 11850.

(8) Upadhyaya, H. P.; Kumar, A.; Naik, P. D. *J. Chem. Phys.* **2003**, *118,* 2590.

(9) Xu, S.; Park, S. T.; Feenstra, J. S.; Srinivasan, R.; Zewail, A. H. *J. Phys. Chem. A* **2004**, *108,* 6650.

(10) Dannenberg, J. J.; Rios, R. *J. Phys. Chem.* **1994**, *98,* 6714.

(11) Delchev, V.; Nikolov, G. *Monatsh. Chem.* **2000**, *131,* 107.

(12) Delchev, V.; Mikosch, H.; Nikolov, G. *Monatsh. Chem.* **2001**, *132,* 331.

(13) Delchev, V.; Mikosch, H. *Russ. J. Phys. Chem.* **2004**, *78,* 1445.

(14) Matanović, I.; Do·slié, N. *J. Phys. Chem. A* **2005**, *109,* 4185.

(15) Nagashima, N.; Kudoh, S.; Takayanagi, M.; Nakata, M. *J. Phys. Chem. A* **2001**, *105,* 10832.

(16) Coussan, S.; Ferro, Y.; Rajzmann, M.; Trivella, A.; Roubin, P.; Wieczorek, R.; Manca, C.; Piecuch, P.; Kowalski, K.; Wloch, M.; Kucharski, S.; Musiał, M. *J. Phys. Chem. A* **2006**, *110,* 3920.

(17) Frisch, M. J.; Trucks, G. W.; Schlegel, H. B.; Scuseria, G. E.; Robb, M. A.; Cheeseman, J. R.; Zakrzewski, V. G.; Montgomery, J. A., Jr.; Stratmann, R. E.; Burant, J. C.; Dapprich, S.; Millam, J. M.; Daniels, A. D.; Kudin, K. N.; Strain, M. C.; Farkas, O.; Tomasi, J.; Barone, V.; Cossi, M.; Cammi, R.; Mennucci, B.; Pomelli, C.; Adamo, C.; Clifford, S.; Ochterski, J.; Petersson, G. A.; Ayala, P. Y.; Cui, Q.; Morokuma, K.; Malick, D. K.; Rabuck, A. D.; Raghavachari, K.; Foresman, J. B.; Cioslowski, J.; Ortiz, J. V.; Stefanov, B. B.; Liu, G.; Liashenko, A.; Piskorz, P.; Komaromi, I.; Gomperts, R.; Martin, R. L.; Fox, D. J.; Keith, T.; Al-Laham, M. A.; Peng, C. Y.; Nanayakkara, A.; Gonzalez, C.; Challacombe, M.; Gill, P. M. W.; Johnson, B. G.; Chen, W.; Wong, M. W.; Andres, J. L.; Head-Gordon, M.; Replogle, E. S.; Pople, J. A. *Gaussian 98*, revision A.2; Gaussian, Inc.: Pittsburgh, PA, 1998.

(18) Allouche, A. *QCPE Bull.* **1993**, *13,* 3.

(19) Allouche, A.; Pourcin, J. *Spectrochim. Acta, Part A* **1993**, *49,* 571.

(20) Coussan, S.; Manca, C.; Ferro, Y.; Roubin, P. *Chem. Phys. Lett.* **2003**, *370,* 118.